

A New Sugar Chain of the Proteinase Inhibitor from Latex of *Carica papaya*¹

Atsuyuki Shimazaki,* Yasushi Makino,* Kaoru Omichi,[†] Shoji Odani,[‡] and Sumihiro Hase*²

*Department of Chemistry, Graduate School of Science, Osaka University, 1-1, Machikaneyama-cho, Toyonaka, Osaka 560-0043; [†]Department of Natural Science, Osaka Women's University, 2-1, Daisen-cho, Sakai, Osaka 590-0035; and [‡]Department of Biology, Faculty of Science, Niigata University, 8050, Igarashininocho, Niigata, Niigata 950-2181

Received November 9, 1998; accepted December 8, 1998

The structure of a sugar chain of the proteinase inhibitor from the latex of *Carica papaya* was studied. Sugar chains liberated on hydrazinolysis were *N*-acetylated, and their reducing-end residues were tagged with 2-aminopyridine. One major sugar chain was detected on size-fractionation and reversed-phase HPLC analyses. The structure of the PA-sugar chain was determined by two-dimensional sugar mapping combined with sequential exoglycosidase digestion and partial acid hydrolysis, and by 750 MHz ¹H-NMR spectroscopy. The structure found was Man α 1-6(Man α 1-3)Man α 1-6(Man α 1-3)(Xyl β 1-2)Man β 1-4GlcNAc β 1-4(Fuc α 1-3)GlcNAc. This sugar chain represents a new plant-type sugar chain with five mannose residues.

Key words: *Carica papaya*, glycoprotein, proteinase inhibitor, sugar chain.

Protein proteinase inhibitors are ubiquitously found in animal and plant tissues. A large number of animal proteinase inhibitors are extracellular proteins functioning in body fluids (1). Plant proteinase inhibitors usually exist in sub-cellular organelles such as protein bodies (2, 3). Recently, an extracellular plant glycoprotein proteinase inhibitor secreted into the latex of green papaya fruit was purified (4). This proteinase inhibitor, which is active against bovine trypsin and α -chymotrypsin, consists of 184 amino acid residues and two *N*-linked sugar chains. Sugar compositional analysis suggested that the sugar chains are composed of mannose, fucose, xylose, and *N*-acetylglucosamine, however, their detailed structures have not yet been determined. Here, we report the sugar structure of the proteinase inhibitor from *Carica papaya*.

MATERIALS AND METHODS

Materials—The proteinase inhibitor from *Carica papaya* was isolated as reported previously (4). PA-isomaltoligosaccharides were purchased from Takara Biomedicals (Kyoto), and jack bean α -mannosidase and *Charonia lampus* α -fucosidase were from Seikagaku Kogyo (Tokyo). Cosmosil 5C18-P columns (0.46 \times 15 cm and 0.15 \times 25 cm)

were obtained from Nacalai Tesque (Kyoto), and a Shodex Asahipak NH2P-50 column (0.46 \times 5 cm) was supplied by Showa Denko (Tokyo). Dowex 50W-X2 (200-400 mesh) was from Dow Chemicals (Richmond, VA), and a TSK gel Sugar AXI column (0.46 \times 15 cm) and TSK gel HW-40F were products of Tosoh (Tokyo).

Standard PA-Sugars—PA-Fuc, PA-Gal, PA-GalNAc, PA-Glc, PA-GlcNAc, PA-Man, PA-Xyl, and PA-isomaltose were previously reported (5). Sugar Chains 1-14, 18, 19, and 22 were prepared as reported (6). The structures and designations of the sugar chains used are listed in Table I.

Preparation of Sugar Chains from the Latex Proteinase Inhibitor—Sugar chains were released from 10 mg of latex proteinase inhibitor by hydrazinolysis (60°C, 50 h) followed by *N*-acetylation under conditions under which *N*- and *O*-linked sugar chains are liberated, and pyridylaminated as described previously (7). The PA-sugar chains were purified by gel filtration on an HW-40F column (1.2 \times 45 cm).

High-Performance Liquid Chromatography—Reversed-phase HPLC was performed on a Cosmosil 5C18-P column (0.46 \times 15 cm) at the flow rate of 1.5 ml/min at 25°C. The column was equilibrated with 0.1 M ammonium acetate buffer, pH 4.0, containing 0.025% 1-butanol. After injecting a sample, the concentration of 1-butanol was increased linearly to 0.5% in 55 min. Elution was monitored by measuring fluorescence (excitation wavelength, 320 nm; emission wavelength, 400 nm).

Reversed-phase HPLC for two-dimensional sugar mapping of the PA-sugar chains was performed on a Cosmosil 5C18-P column (0.15 \times 25 cm) at the flow rate of 150 μ l/min at 25°C. The column was equilibrated with 20 mM ammonium acetate buffer, pH 4.0, containing 0.075% 1-butanol. After injecting a sample, the concentration of 1-butanol was increased linearly to 0.4% in 90 min. PA-sugar chains were detected as described above. Their elution

¹ This work was supported in part by a Grant-in-Aid for Scientific Research from the Ministry of Education, Science, Sports and Culture of Japan.

² To whom correspondence should be addressed.

Abbreviations: Fuc, fucose; Gal, galactose; GalNAc, *N*-acetylgalactosamine; Glc, glucose; GlcNAc, *N*-acetylglucosamine; Man, mannose; PA-, pyridylamino; Xyl, xylose. All sugars mentioned in this paper except fucose were of the D-series. TOCSY, total correlated spectroscopy.

TABLE I. Structures and designations of pyridylaminated sugar chains used in this study.

Structure	Sugar Chain	Structure	Sugar Chain
$\begin{array}{c} \text{Man}\beta 1 - 4\text{GlcNAc}\beta 1 - 4\text{GlcNAc} - \text{PA} \\ \\ \text{Xyl}\beta 1 \end{array}$	1	$\begin{array}{c} \text{Man}\alpha 1 - 3 \text{Man}\alpha 1 - 6 \text{Man}\beta 1 - 4\text{GlcNAc}\beta 1 - 4\text{GlcNAc} - \text{PA} \\ \\ \text{Xyl}\beta 1 \end{array}$	15
$\begin{array}{c} \text{Man}\beta 1 - 4\text{GlcNAc}\beta 1 - 4\text{GlcNAc} - \text{PA} \\ \\ \text{Xyl}\beta 1 \end{array}$	2	$\begin{array}{c} \text{Man}\alpha 1 - 6 \text{Man}\alpha 1 - 6 \text{Man}\beta 1 - 4\text{GlcNAc}\beta 1 - 4\text{GlcNAc} - \text{PA} \\ \\ \text{Xyl}\beta 1 \end{array}$	16
$\text{GlcNAc}\beta 1 - 4\text{GlcNAc} - \text{PA}$	3	$\begin{array}{c} \text{Man}\alpha 1 - 6 \text{Man}\alpha 1 - 3 \text{Man}\beta 1 - 4\text{GlcNAc}\beta 1 - 4\text{GlcNAc} - \text{PA} \\ \\ \text{Xyl}\beta 1 \end{array}$	17
$\text{Man}\beta 1 - 4\text{GlcNAc}\beta 1 - 4\text{GlcNAc} - \text{PA}$	4	$\begin{array}{c} \text{Man}\alpha 1 - 3 \text{Man}\beta 1 - 4\text{GlcNAc}\beta 1 - 4\text{GlcNAc} - \text{PA} \\ \\ \text{Xyl}\beta 1 \end{array}$	18
$\text{Man}\alpha 1 - 3 \text{Man}\beta 1 - 4\text{GlcNAc}\beta 1 - 4\text{GlcNAc} - \text{PA}$	5	$\begin{array}{c} \text{Man}\alpha 1 - 6 \text{Man}\alpha 1 - 3 \text{Man}\beta 1 - 4\text{GlcNAc}\beta 1 - 4\text{GlcNAc} - \text{PA} \\ \\ \text{Xyl}\beta 1 \end{array}$	19
$\text{Man}\alpha 1 - 6 \text{Man}\beta 1 - 4\text{GlcNAc}\beta 1 - 4\text{GlcNAc} - \text{PA}$	6	$\begin{array}{c} \text{Man}\alpha 1 - 6 \text{Man}\alpha 1 - 6 \text{Man}\beta 1 - 4\text{GlcNAc}\beta 1 - 4\text{GlcNAc} - \text{PA} \\ \\ \text{Xyl}\beta 1 \end{array}$	20
$\text{Man}\alpha 1 - 3 \text{Man}\alpha 1 - 6 \text{Man}\beta 1 - 4\text{GlcNAc}\beta 1 - 4\text{GlcNAc} - \text{PA}$	7	$\begin{array}{c} \text{Man}\alpha 1 - 6 \text{Man}\alpha 1 - 3 \text{Man}\beta 1 - 4\text{GlcNAc}\beta 1 - 4\text{GlcNAc} - \text{PA} \\ \\ \text{Xyl}\beta 1 \end{array}$	21
$\text{Man}\alpha 1 - 6 \text{Man}\alpha 1 - 6 \text{Man}\beta 1 - 4\text{GlcNAc}\beta 1 - 4\text{GlcNAc} - \text{PA}$	8	$\begin{array}{c} \text{Man}\alpha 1 - 6 \text{Man}\alpha 1 - 3 \text{Man}\beta 1 - 4\text{GlcNAc}\beta 1 - 4\text{GlcNAc} - \text{PA} \\ \\ \text{Xyl}\beta 1 \end{array}$	22
$\text{Man}\alpha 1 - 6 \text{Man}\beta 1 - 4\text{GlcNAc}\beta 1 - 4\text{GlcNAc} - \text{PA}$	9		
$\text{Man}\alpha 1 - 6 \text{Man}\beta 1 - 4\text{GlcNAc}\beta 1 - 4\text{GlcNAc} - \text{PA}$	10		
$\text{Man}\alpha 1 - 6 \text{Man}\alpha 1 - 6 \text{Man}\beta 1 - 4\text{GlcNAc}\beta 1 - 4\text{GlcNAc} - \text{PA}$	11		
$\text{Man}\alpha 1 - 6 \text{Man}\alpha 1 - 3 \text{Man}\beta 1 - 4\text{GlcNAc}\beta 1 - 4\text{GlcNAc} - \text{PA}$	12		
$\text{Man}\alpha 1 - 3 \text{Man}\alpha 1 - 6 \text{Man}\beta 1 - 4\text{GlcNAc}\beta 1 - 4\text{GlcNAc} - \text{PA}$	13		
$\text{Man}\alpha 1 - 6 \text{Man}\beta 1 - 4\text{GlcNAc}\beta 1 - 4\text{GlcNAc} - \text{PA}$	14		

positions were expressed as *R* values according to the reversed-phase scale previously reported (6).

Size-fractionation HPLC was performed on a Shodex NH2P-50 column (0.46 × 5 cm) at the flow rate of 0.6 ml/min at 25°C using two eluents. Eluent A was 0.3% (v/v) acetic acid in a 1:4 (v/v) mixture of acetonitrile:water adjusted to pH 7.0 with aqueous ammonia, and Eluent B was 0.3% (v/v) acetic acid in a 93:7 (v/v) mixture of acetonitrile:water adjusted to pH 7.0 with aqueous ammonia. The column was equilibrated with a 3:97 (v/v) mixture of Eluent A:Eluent B. After injecting a sample, the proportion of Eluent A was increased linearly to 33% in 1 min, and then to 71% in 34 min. Elution was monitored by measuring the fluorescence (excitation wavelength, 310 nm; emission

wavelength 380 nm). The elution positions of the PA-sugar chains were expressed as glucose units using PA-isomaltoligosaccharides.

Reducing-End Analysis of PA-Sugar Chains—The PA-sugar chains to be analyzed (20 pmol) were hydrolyzed with 4 M hydrochloric acid at 100°C for 8 h, followed by *N*-acetylation. PA-monosaccharides were analyzed by TSK gel Sugar AXI HPLC (8).

Exoglycosidase Digestion of PA-Sugar Chains—A PA-sugar chain to be analyzed (150 pmol) was digested with 0.4 unit of α -mannosidase in 40 μ l of 40 mM sodium citrate buffer, pH 4.5, at 37°C for 17 h, and then with 5 milliunits of α -fucosidase in 35 μ l 0.1 M ammonium acetate buffer, pH 3.9, at 37°C for 24 h. The enzymatic reaction was

terminated by heating the solution at 100°C for 3 min.

Analysis of Oligosaccharide Structures from the Reducing-End Terminal (9)—To 200 pmol of a PA-sugar chain, 200 μ l of a 1 M trifluoroacetic acid aqueous solution was added, and half the mixture was hydrolyzed at 100°C for 10 min and the other half for 1 h. The combined hydrolysates were freeze-dried, followed by *N*-acetylation. The sample obtained was size-fractionated every 1 glucose unit using PA-isomaltooligosaccharides as an elution scale. After lyophilization of each fraction, the fractions were analyzed by reversed-phase HPLC.

NMR Spectroscopy—Prior to NMR spectroscopic analysis, a sample was exchanged twice in 99.96% D₂O (Matheson, USA) with intermediate lyophilization. Finally, the sample was dissolved in 600 μ l of 99.96% D₂O.

The TOCSY spectrum at 750 MHz was recorded using a Varian Unity Inova 750 MHz NMR spectrometer with a mixing sequence of 120 ms, the spin-lock field strength corresponding to a 90° pulse width of 42.0 μ s. Measurements were made at 30°C. Signals under the HOD peak were detected by carrying out the measurements at 50°C.

RESULTS AND DISCUSSION

Separation and Reducing-End Analysis of PA-Sugar Chains from the Latex Proteinase Inhibitor—PA-sugar chains obtained from the latex proteinase inhibitor of *C. papaya* were separated by reversed-phase HPLC (Fig. 1). Size-fractionation HPLC and reducing-end analysis revealed that Fraction D was a single component, its molecular size was 8.1 glucose units, and its reducing-end residue was PA-GlcNAc. The molecular size of Fraction C was 8.0 glucose unit, and its reducing-end residue was PA-ManNAc (data not shown). Therefore, Fraction C was probably a by-product of Fraction D formed during preparation, as usually found (10). Size-fractionation HPLC and reducing-end analysis of Fractions A and B indicated that they were contaminating materials, and these peaks were usually observed for the peptide portion (11). From these results, it was inferred that the proteinase inhibitor has only one major *N*-linked sugar chain structure.

Two-Dimensional Sugar Mapping of a Sequential Exoglycosidase Digest of Fraction D—Fraction D was not identified as one of the authentic PA-sugar chains on a two-dimensional sugar map obtained with the combination of size-fractionation and reversed-phase HPLC. Fraction D was then digested with α -mannosidase (arrow a in Fig. 2), and the elution position of the product was found to be

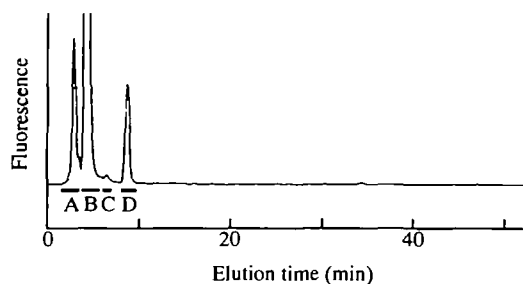


Fig. 1. Separation by reversed-phase HPLC of PA-sugar chains from the latex proteinase inhibitor. Fractions were pooled as indicated by the bars.

identical to that of Sugar Chain 1. This digestion reduced the molecular size from 8.1 to 3.7 glucose units, indicating the removal of four mannose residues. Further digestion of the product with α -fucosidase resulted in the appearance of a new peak at the position of Sugar Chain 2 (arrow b in Fig. 2). These results suggested that the structure of Fraction D was Man₄(Xyl β 1-2)Man β 1-4GlcNAc β 1-4(Fuc α 1-3)GlcNAc-PA.

Structural Analysis of Fraction D from the Reducing-End Terminal—The structure of Fraction D was analyzed from the reducing-end terminal by combining partial acid hydrolysis and two-dimensional sugar mapping (9). The results of size-fractionation HPLC are shown in Fig. 3. Only PA-GlcNAc was detected in Fraction D1 on anion-exchange HPLC on a TSK gel Sugar AXI column (data not shown).

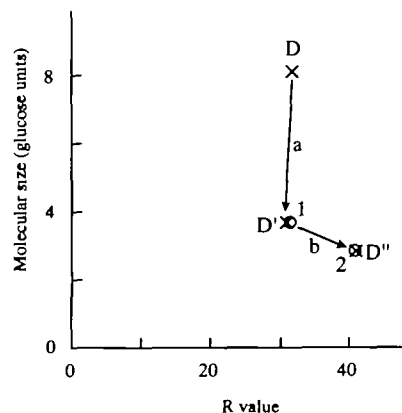


Fig. 2. Two-dimensional HPLC mapping of Fraction D and its sequential digest with exoglycosidases. The molecular sizes of PA-oligosaccharides are plotted on the ordinate in terms of glucose units using PA-isomaltooligosaccharides. On the abscissa, the elution positions of PA-oligosaccharides on reversed-phase HPLC are shown in terms of the *R* values (6). The abbreviations and the structures of the PA-oligosaccharides are listed in Table I. Open circles represent the elution positions of authentic Sugar Chains 1 and 2, and Xs the elution positions of D, D', and D''. D' is the digest of Fraction D with α -mannosidase, and D'' is the digest of D' with α -fucosidase. Arrows a and b, respectively, indicate the digests with α -mannosidase and α -fucosidase.

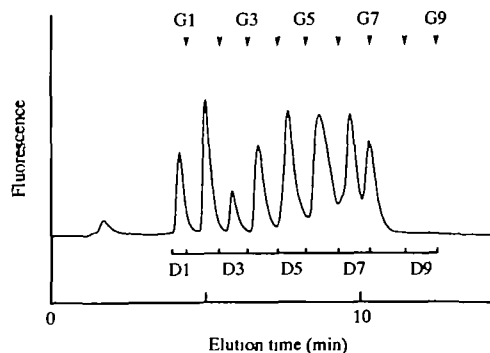


Fig. 3. Size-fractionation HPLC of the partial acid hydrolysate of Fraction D. PA-oligosaccharides were fractionated on a Shodex NH2P-50 column. Arrowheads G1-G9 indicate the elution positions of PA-isomaltooligosaccharides. Fractions were pooled as indicated by bars D1-D9. The peaks that appeared at around 2 min were due to contaminating materials.

The other fractions were analyzed by reversed-phase HPLC (Fig. 4). Sugar Chains 3 and 4 were detected in Fractions D2 and D3, respectively. In Fraction D4, Sugar Chains 5 and 6 were detected. These findings suggested that Fraction D5 might contain Sugar Chain 9, which was in fact confirmed by Peak 9 (Fig. 4-D5). From the detection of Sugar Chain 7 or 8 in Fraction D5 and the presence of five mannose residues in Fraction D, it was predicted that Fraction D7 should contain Sugar Chain 19, which was in fact Peak 19. The structure of Sugar Chain 19 in Fraction D was further confirmed by identifying PA-sugar chain fragments (the black peaks in Fig. 4) derived from authentic Sugar Chain 19 by applying the same procedure. The presence of Sugar Chains 15 or 16, and 14 in Fraction D6 signified that Fraction D8 should contain Sugar Chain 21, which was in fact Peak 21. The estimated structure of Sugar Chain 21 in Fraction D was confirmed by identifying all the peaks for possible fragments derived theoretically from Sugar Chain 21. The absence of a peak at the elution position of Fraction D (Fig. 4-D9) indicated that Fraction D had an acid-labile substituent such as a fucose or sialic acid residue, the difference in the elution position between D and Peak 21 being characteristic of a $\text{Fuc}\alpha 1-3$ residue (6). On the basis of these results, we postulated that Fraction D had the structure, $\text{Man}\alpha 1-6(\text{Man}\alpha 1-3)\text{Man}\alpha 1-6(\text{Man}\alpha 1-3)(\text{Xyl}\beta 1-2)\text{Man}\beta 1-4\text{GlcNAc}\beta 1-4(\text{Fuc}\alpha 1-3)\text{GlcNAc-PA}$.

Structure Analysis of Fraction D by $^1\text{H-NMR}$ Spectroscopy—To confirm the postulated structure of Fraction D, additional evidence was obtained by 750 MHz $^1\text{H-NMR}$ spectroscopy. Part of the TOCSY spectrum and part of the one-dimensional spectrum are shown in Fig. 5A. By carrying out the measurements at 50°C, we confirmed that there

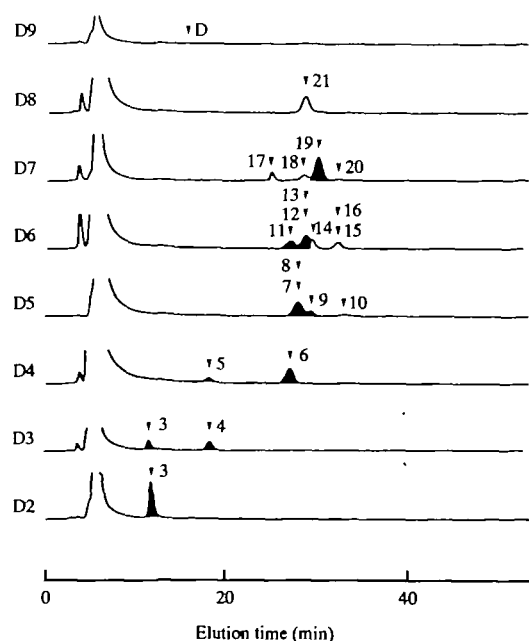


Fig. 4. Reversed-phase HPLC analysis of Fractions D2-D9. Black arrowheads indicate the elution positions of authentic PA-sugar chains, and white arrowheads show the calculated elution positions of non-standard PA-sugar chains as reported (6). The peaks that appeared at around 5 min are due to contaminating materials. The numbers and designations of the sugar chains used are listed in Table I.

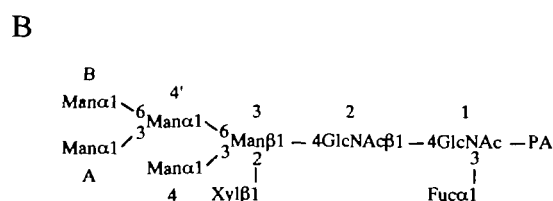
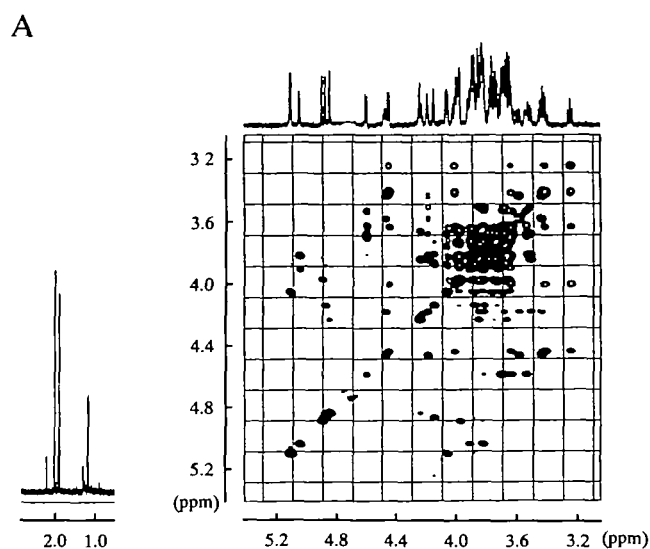


Fig. 5. $^1\text{H-NMR}$ analysis of Fraction D and the proposed structure of Fraction D from the latex proteinase inhibitor. (A) Part of the TOCSY spectrum recorded at 30°C and part of the one-dimensional spectrum of Fraction D. (B) Proposed structure of Fraction D and coding of the sugar residues used in this paper.

TABLE II. Chemical shifts (ppm) of structural reporter groups of PA-sugar chains analyzed by 750 MHz $^1\text{H-NMR}$ spectroscopy. NMR spectroscopic analysis was performed at 30 and 50°C (signals shown in parentheses). Chemical shifts are expressed in ppm using internal acetone ($\delta = 2.218$ and 2.213 ppm) in D_2O at 30 and 50°C, respectively. Coupling constant, $J_{1,2}$, values at 30°C are shown in angle brackets.

	Fraction D	Sugar chain 22 ^b	Sugar chain 19 ^c
CH_3 of Fuc	1.194 (1.190)	1.206	
CH_3 of NAc 1	1.921 (1.924)	1.934	1.949
CH_3 of NAc 2	2.033 (2.029)	2.056	2.064
H-1 of 2	4.591 (4.597)	[4.630] ^a	4.645
	<8.1>		
H-1 of Fuc	5.043 (5.036)	5.060	
	<4.1>		
H-1 of Xyl	4.442	4.452	
	<7.2>		
H-1 of 3	4.842 (4.830)	[4.843] ^a	4.784
H-1 of 4	5.107 (5.115)	5.135	5.107
H-1 of 4'	4.870 (4.870)	4.925	4.878
H-1 of A	5.103 (5.100)		5.102
H-1 of B	4.894 (4.894)		4.913
H-2 of 3	4.236 (4.233)	4.270	4.242
H-2 of 4	4.055 (4.054)	4.050	4.083
H-2 of 4'	4.143 (4.132)	4.000	4.152
H-2 of A	4.055 (4.054)		4.069
H-2 of B	3.972 (3.897)		3.987

^aData for 65°C in square brackets; ^bdata from Ref. 12; ^cdata from Ref. 22.

were no signals under the HOD peak at 30°C. The chemical shifts of the structural reporter groups of Fraction D were compared with those reported previously for Sugar Chains 19 and 22 (Table II). The coding of the sugar residues used is shown in Fig. 5B.

The signals at 1.194, 1.921, and 2.033 ppm were assigned to the methyl protons of Fuc, GlcNAc-1, and GlcNAc-2, respectively. The anomeric proton signal ($\delta = 4.591$ ppm) was assigned to GlcNAc-2, because its chemical shift was similar to that of Sugar Chain 22 and the large coupling constant (8.1 Hz) indicated a β -linkage. The chemical shift of the anomeric proton of Man-3 was almost the same as that of Sugar Chain 22. The signals at $\delta = 5.043$ and 4.442 ppm, in combination with the coupling constants $J_{1,2}$ (4.1 and 7.2 Hz), were typical signals of Fuc α 1-3 and Xyl β 1-2 residues, respectively, as found in Sugar Chain 22. The other anomeric proton signals, at 5.107, 4.870, 5.103, and 4.894 ppm, were similar to those of Sugar Chain 19, and thus were assigned to Man-4, Man-4', Man-A, and Man-B, respectively. These NMR results further confirmed the findings obtained on exoglycosidase digestion and partial acid hydrolysis.

Structure of the Sugar Chains in the Latex Proteinase Inhibitor—On the basis of the results described above, the structure of the sugar chain in the latex proteinase inhibitor from *C. papaya* was determined (Fig. 5B). The results were compatible with the sugar composition of the glycoprotein reported previously (4). Plant-type *N*-linked sugar chains with Fuc α 1-3 and Xyl β 1-2 residues in their high-mannose structures have been reported, and Sugar Chain 22 is typical of such a structure (12–15). However, Man α 1-6(Man α 1-3)Man α 1-6(Man α 1-3)(Xyl β 1-2)Man β 1-4GlcNAc β 1-4(Fuc α 1-3)GlcNAc has not so far been reported to our knowledge. It is also noteworthy that the latex proteinase inhibitor from *C. papaya* has only one sugar chain, since microheterogeneity of sugar chains is found in most glycoproteins.

In the reported biosynthetic pathway for plant-type *N*-linked sugar chains with fucose and xylose residues, a xylosyltransferase transfers xylose to a sugar chain after the removal of Man-A and Man-B by Golgi α -mannosidase

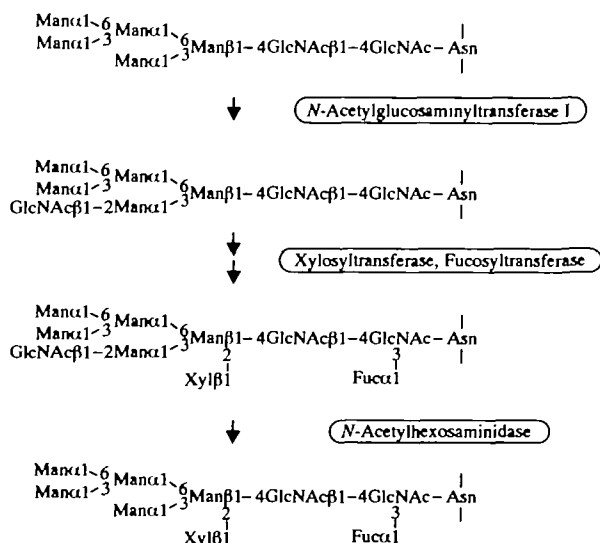


Fig. 6. Possible biosynthetic pathway for Fraction D.

II (16–18). However, a few plant sugar chains, such as Man α 1-3Man α 1-6(Man α 1-3)(Xyl β 1-2)Man β 1-4GlcNAc β 1-4GlcNAc (19), Man α 1-6(Man α 1-3)Man α 1-6(GlcNAc β 1-2Man α 1-3)(Xyl β 1-2)Man β 1-4GlcNAc β 1-4GlcNAc (20), and Man α 1-3/6Man α 1-6(Man α 1-3)(Xyl β 1-2)Man β 1-4GlcNAc β 1-4(Fuc α 1-3)GlcNAc (21), are not consistent with the above biosynthetic pathway. These reported results and the finding of Fraction D in this study may indicate that Golgi α -mannosidase II did not act on this glycoprotein, as shown in Fig. 6. This pathway may be possible because the xylosyltransferase can transfer xylose to Man α 1-6(Man α 1-3)Man α 1-6(GlcNAc β 1-2Man α 1-3)-Man β 1-4GlcNAc β 1-4GlcNAc, although the activity is low (16, 17).

We wish to thank Dr. K. Lee (Osaka University, Graduate School of Science) for the operation of and technical advice on the Varian Unity 750 MHz NMR spectrometer of the Venture Business Laboratory, Osaka University.

REFERENCES

- Carrell, R.W. and Boswell, D.R. (1986) Serpins: the superfamily of plasma serine proteinase inhibitors in *Proteinase Inhibitors* (Barrett, A.J., and Salvesen, G., eds.) pp. 403–420, Elsevier, Amsterdam
- Koide, T. and Ikenaka, T. (1973) Studies on soybean trypsin inhibitors. *Eur. J. Biochem.* **32**, 417–431
- Graham, J.S., Pearce, G., Merryweather, J., Titani, K., Ericsson, L., and Ryan, C.A. (1985) Wound-induced proteinase inhibitors from tomato leaves. *J. Biol. Chem.* **260**, 6555–6560
- Odani, S., Yokokawa, Y., Takeda, H., Abe, S., and Odani, S. (1996) The primary structure and characterization of carbohydrate chains of the extracellular glycoprotein proteinase inhibitor from latex of *Carica papaya*. *Eur. J. Biochem.* **241**, 77–82
- Makino, Y., Kuraya, N., Omichi, K., and Hase, S. (1996) Classification of sugar chains of glycoproteins by analyzing reducing end oligosaccharides obtained by partial acid hydrolysis. *Anal. Biochem.* **238**, 54–59
- Yanagida, K., Ogawa, H., Omichi, K., and Hase, S. (1998) Introduction of a new scale into reversed-phase high-performance liquid chromatography of pyridylamino sugar chains for structural assignment. *J. Chromatogr. A* **800**, 187–198
- Kuraya, N. and Hase, S. (1992) Release of *O*-linked sugar chains from glycoproteins with anhydrous hydrazine and pyridylation of the sugar chains with improved reaction conditions. *J. Biochem.* **112**, 122–126
- Hase, S., Hatanaka, K., Ochiai, K., and Shimizu, H. (1992) Improved method for the component sugar analysis of glycoproteins by pyridylamino sugars purified with immobilized boronic acid. *Biosci. Biotechnol. Biochem.* **56**, 1676–1677
- Makino, Y., Omichi, K., and Hase, S. (1998) Analysis of oligosaccharide structures from the reducing end terminal by combining partial acid hydrolysis and a two-dimensional sugar map. *Anal. Biochem.* **264**, 172–179
- Hase, S., Ibuki, T., and Ikenaka, T. (1984) Reexamination of the pyridylation used for fluorescence labeling of oligosaccharides and its application to glycoproteins. *J. Biochem.* **95**, 197–203
- Hase, S., Ikenaka, T., and Matsushima, Y. (1981) A highly sensitive method for analyses of sugar moieties of glycoproteins by fluorescence labeling. *J. Biochem.* **90**, 407–414
- Hase, S., Koyama, S., Daiyasu, H., Takemoto, H., Hara, S., Kobayashi, Y., Kyogoku, Y., and Ikenaka, T. (1986) Structure of a sugar chain of a proteinase inhibitor isolated from Barbados Pride (*Caesalpinia pulcherrima* Sw.) seeds. *J. Biochem.* **100**, 1–10
- Takahashi, N., Hitotsuya, H., Hanzawa, H., Arata, Y., and Kurihara, Y. (1990) Structural study of asparagine-linked oligosaccharide moiety of taste-modifying protein, Miraculin. *J. Biol. Chem.* **265**, 7793–7798

14. Kimura, Y., Yamaguchi, K., and Funatsu, G. (1996) Structural analysis of *N*-linked oligosaccharide of mitogenic lectin-B from the roots of pokeweed (*Phytolacca americana*). *Biosci. Biotechnol. Biochem.* **60**, 537-540
15. Strum, A., Bergwerff, A.A., and Vliegthart, F.G. (1992) ¹H-NMR structural determination of the *N*-linked carbohydrate chains on glycopeptides obtained from the bean lectin *phytohemagglutinin*. *Eur. J. Biochem.* **204**, 313-316
16. Johnson, K.D. and Chrispeels, M.J. (1987) Substrate specificities of *N*-acetylglucosaminyl-, fucosyl-, and xylosyltransferases that modify glycoproteins in the Golgi apparatus of bean cotyledons. *Plant. Physiol.* **84**, 1301-1308
17. Tezuka, K., Hayashi, M., Ishihara, H., Akazawa, T., and Takahashi, N. (1992) Studies on synthetic pathway of xylose-containing *N*-linked oligosaccharides deduced from substrate specificities of the processing enzymes in sycamore cells (*Acer pseudoplatanus* L.). *Eur. J. Biochem.* **203**, 401-413
18. Faye, L., Johnson, K.D., Sturm, A., and Chrispeels, M.J. (1989) Structure, biosynthesis, and function of asparagine-linked glycans on plant glycoproteins. *Physiol. Plant.* **75**, 309-314
19. Kimura, Y., Hase, S., Kobayashi, Y., Kyogoku, Y., Funatsu, G., and Ikenaka, T. (1987) Possible pathway for the processing of sugar chains containing xylose in plant glycoproteins deduced on structural analysis of sugar chains from *Ricinus communis* lectins. *J. Biochem.* **101**, 1051-1054
20. Oxley, D., Munro, S.L.A., Craik, D.J., and Bacic, A. (1998) Structure and distribution of *N*-glycans on the *S₇*-allele stylar self-incompatibility ribonuclease of *Nicotiana glauca*. *J. Biochem.* **123**, 978-983
21. Altmann, F., Paschinger, K., Dalik, T., and Vorauer, K. (1998) Characterization of peptide-*N*⁴-(*N*-acetyl- β -glucosaminyl)asparagine amidase A and its *N*-glycans. *Eur. J. Biochem.* **252**, 118-123
22. Koyama, S., Daiyasu, H., Hase, S., Kobayashi, Y., Kyogoku, Y., and Ikenaka, T. (1986) ¹H-NMR analysis of the sugar structures of glycoproteins as their pyridylamino derivatives. *FEBS Lett.* **209**, 265-268